

# Scattering of two photons on a quantum emitter in a one-dimensional waveguide: Exact dynamics and induced correlations

Anders Nysteen, Philip Trøst Kristensen, Dara P. S. McCutcheon, Per Kaer, and Jesper Mørk

DTU Fotonik, Department of Photonics Engineering, Ørstedes Plads, 2800 Kgs Lyngby, Denmark

E-mail: anys@fotonik.dtu.dk

**Abstract.** We develop a wavefunction approach to describe the scattering of two photons on a quantum emitter embedded in a one-dimensional waveguide. Our method allows us to calculate the exact dynamics of the complete system at all times, as well as the transmission properties of the emitter. We show that the non-linearity of the emitter with respect to incoming photons depends strongly on the emitter excitation and the spectral shape of the incoming pulses, resulting in transmission of the photons which depends crucially on their separation and width. In addition, for counter-propagating pulses, we analyze the induced level of quantum correlations in the scattered state, and we show that the emitter behaves as a non-linear beam-splitter when the spectral width of the photon pulses is similar to the emitter decay rate.

## 1. Introduction

Single photons play an important role in many of the rapidly emerging quantum technologies [1, 2], including quantum communication [3], quantum metrology [4], and optical quantum information processing [5]. The most ambitious of these technologies require the manipulation of data encoded in the state of the photons, necessitating both single and two-photon gates [5, 6, 7]. Whilst single-photon gates can be readily implemented with passive linear optical components, photons do not inherently interact, and two-photon gates therefore typically require non-linear components [7]. Owing to the usually weak nature of these non-linearities, their utilisation at the few-photon level represents a significant challenge.

Significant progress has been made, however, by utilising the relatively strong light-matter interaction between photons and semiconductor quantum dots [8, 9, 10]. The idea is to use these nano-structures as ‘third-parties’, in order to achieve an effective interaction between two otherwise non-interacting photons. Additionally, quantum dots can be placed in various structures to allow for guidance of the incoming and outgoing photons. These setups include quantum dots in photonic nanowires [2], close to plasmonic waveguides [11, 12], and inside line defects of photonic crystal waveguide slabs (PCWS) [13]. The last of these systems opens up the intriguing possibility of all-optical on-chip integrated circuits [1, 14], with the demonstration of extremely high coupling efficiencies between quantum dots and waveguide modes having recently been achieved [15], as too has the precise positioning of quantum dots on substrates thanks to improvements in fabrication techniques [16].

The dynamics of a quantum two-level emitter (TLE) interacting with single-photon wavepackets of infinitely narrow bandwidth in a photonic waveguide is well understood. In this scenario, the emitter does not become appreciably populated, and the resulting dynamical (Markovian) equations can be solved. Notably, scattering on a resonant TLE results in total reflection due to destructive interference between the scattered field and the incoming field on the transmission side of the TLE [17, 18]. Intrinsic losses, such as phonon coupling and other non-radiative processes are known to deteriorate this complete destructive interference effect [19], as too does decay of the emitter into modes other than the guided mode. Deviations are also expected for scattering of non-monochromatic photon pulses when the finite width of the incoming pulses is taken into account, resulting in non-zero transmission [20].

The scattering of multiple photons with finite bandwidth is much more complicated, as the non-linear emitter can induce correlations between the photons caused by elastic multi-photon scattering processes [21, 22]. Existing methods for analyzing the multiple-photon scattering problem — such as the input-output formalism [22], the real-space Bethe ansatz [23], or the Lehmann-Symanzik-Zimmermann formalism [24] — focus on the long-time limit of the scattered state [25] and necessitate the computation of complicated scattering elements. Some specific considerations have been demonstrated using a wavefunction description of the system [26], e.g. the demonstration of stimulated emission of an emitter inside a waveguide [27], and scattering of a two-photon wavepacket in a photonic tight-binding waveguide [28, 29]. Applications which utilize a TLE nonlinearity have been proposed, such as photon sorters and Bell state analyzers [30]. In all these cases the non-linearity of the emitter leads to rich scattering dynamics and scattering-induced correlations. It is the interplay between these highly non-trivial scattering properties and the excitation dynamics of the emitter which we seek to clarify in this work.

To do so we study two-photon scattering on a quantum emitter in a one-dimensional waveguide using a wavefunction approach, in which the entire system state is explicitly calculated at all times during the scattering process, and which therefore provides a detailed picture of the scattering dynamics. This approach relies on a direct solution of the Schrödinger equation by expanding the complete state in a basis formed by the TLE and the optical waveguide modes. This allows us to explore varying widths and separations of the incoming photons, and provides a convenient and detailed visualization of the temporal dynamics of the scattering process. As a special case, we show that the approach agrees with the above-mentioned methods in the post-scattering limit. For co-propagating pulses, we find that the transmission properties of the emitter depend crucially on the pulse width and separation, with closer spaced pulses giving rise to a larger proportion of scattered light. For counter-propagating coincident pulses we find that the emitter behaves as a non-linear beam-splitter, and we investigate the quantum correlations induced in the scattered photonic state.

This paper is structured as follows: In section 2 we introduce the model and formalism. In section 3 we analyse the scattering dynamics for two co-propagating photon pulses; we examine how the properties of the scattered state depend on the emitter excitation and consider the scattering-induced correlations between the photons. In section 4 we study scattering of counter-propagating pulses, elucidating the analogy of the quantum emitter and a non-linear beam-splitter. Finally, in section 5 we summarise our results.

## 2. The model

The model we study consists of a TLE coupled to an infinite one-dimensional waveguide with modes propagating in both directions. This model could be realized, for example, by a line defect in a photonic crystal containing a quantum dot, as depicted in Fig. 1. The complete Schrödinger picture Hamiltonian reads  $H = H_0 + H_I$ , where  $H_0 = \hbar\omega_0 c^\dagger c + \sum_\lambda \hbar\omega_\lambda a_\lambda^\dagger a_\lambda$  and  $H_I = \hbar \sum_\lambda [g_\lambda a_\lambda c^\dagger + g_\lambda^* a_\lambda^\dagger c]$ , in which  $\lambda$  is a generalised quantum number describing polarisation

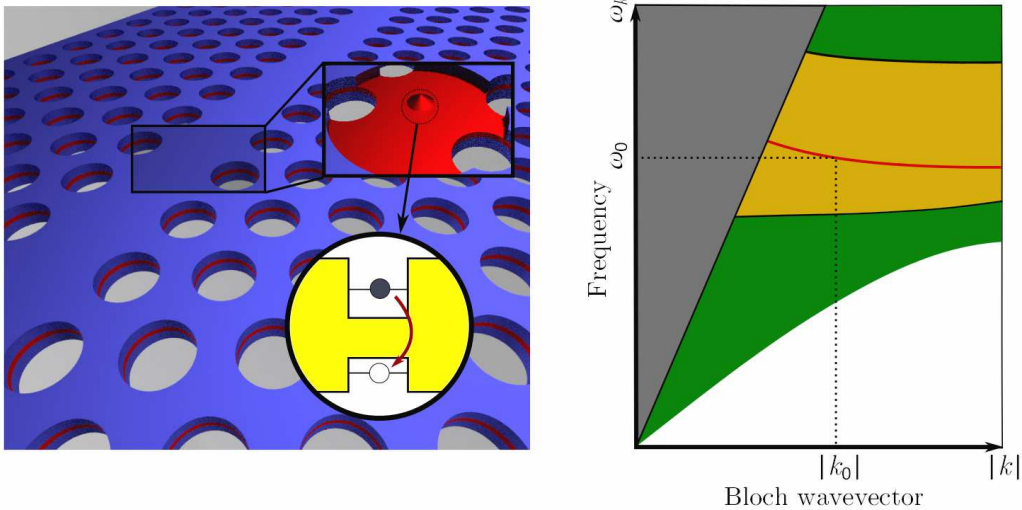


**Figure 1.** (Left) Illustration of a TLE embedded in a one-dimensional waveguide, exemplified by a line defect in a photonic crystal slab containing a quantum dot. (Right) Schematic illustration of the corresponding band diagram showing the slab modes (green area) with a bandgap (yellow area) containing a line defect mode (red line). The resonance frequency of the emitter,  $\omega_0$ , lies inside the bandgap, and we consider only propagating modes below the light cone (shaded grey).

and propagation degrees of freedom, and each mode is described by creation and annihilation operators  $a_\lambda^\dagger$  and  $a_\lambda$ , respectively. The TLE is described by creation and annihilation operators  $c^\dagger$  and  $c$  and has excited state energy  $\hbar\omega_0$ . The coupling between the TLE and mode  $\lambda$  is  $g_\lambda$ .

Moving into a rotating frame described by the transformation  $T(t) = \exp[-i\omega_0(c^\dagger c + \sum_\lambda a_\lambda^\dagger a_\lambda)]$ , we find the transformed Hamiltonian  $\tilde{H} = T^\dagger(t)HT(t) + i\hbar\frac{\partial T^\dagger}{\partial t}T(t) = \tilde{H}_0 + \tilde{H}_I$  where

$$\tilde{H}_0 = \sum_\lambda \hbar\Delta\omega_\lambda a_\lambda^\dagger a_\lambda, \quad \text{and} \quad \tilde{H}_I = H_I = \hbar \sum_\lambda \left[ g_\lambda a_\lambda c^\dagger + g_\lambda^* a_\lambda^\dagger c \right], \quad (1)$$

where  $\Delta\omega_\lambda = \omega_\lambda - \omega_0$  is the detuning of mode  $\lambda$  from the TLE emitter transition energy. From this point onwards we work exclusively in this rotating frame.

### 2.1. Dynamics

For photonic applications, the TLE would ideally couple exclusively to guided modes in the waveguide, leading to a lossless system in which the number of excitations is strictly conserved. We note that recent experimental work has shown coupling of a quantum dot to modes in a one-dimensional waveguide with an efficiency of up to 98% [15]. In our analysis we therefore assume coupling only to the waveguide modes, which allows us to expand a general state of the system in a basis spanned by the states  $|g, \lambda_1 \lambda_2\rangle$  and  $|e, \lambda\rangle$ , where the first index refers to the TLE in the ground (g) or excited (e) state, and the second index labels the population of the waveguide mode(s). We note that since the photons are fundamentally indistinguishable, the states  $|g, \lambda_1 \lambda_2\rangle$  and  $|g, \lambda_2 \lambda_1\rangle$  are equivalent.

We write the total state at time  $t$  as

$$|\psi(t)\rangle = \frac{1}{\sqrt{2}} \sum_{\lambda_1 \lambda_2} C_{\lambda_1 \lambda_2}^g(t) a_{\lambda_1}^\dagger a_{\lambda_2}^\dagger |g, 0\rangle + \sum_\lambda C_\lambda^e(t) a_\lambda^\dagger |e, 0\rangle, \quad (2)$$

where the expansion coefficients  $C_{\lambda_1\lambda_2}^g(t)$  and  $C_\lambda^e(t)$  are in the rotating frame, and  $|0\rangle$  indicates the vacuum state of the waveguide. Since  $[a_{\lambda_1}^\dagger, a_{\lambda_2}^\dagger] = 0$  (and indeed  $|g, \lambda_1\lambda_2\rangle = |g, \lambda_2\lambda_1\rangle$ ), the coefficients of the two-photon terms must be symmetric,  $C_{\lambda_1\lambda_2}^g(t) = C_{\lambda_2\lambda_1}^g(t)$ . Normalization of the state requires  $\langle\psi(t)|\psi(t)\rangle = \sum_{\lambda_1,\lambda_2} |C_{\lambda_1\lambda_2}^g(t)|^2 + \sum_\lambda |C_\lambda^e(t)|^2 = 1$ , and we can interpret  $\sum_\lambda |C_\lambda^e(t)|^2$  as the probability that the TLE is measured in its excited state, while the probability of measuring two photons in modes  $\lambda_1$  and  $\lambda_2$  for  $\lambda_1 \neq \lambda_2$  is  $2|C_{\lambda_1\lambda_2}^g(t)|^2$ , and  $|C_{\lambda_1\lambda_1}^g(t)|^2$  for  $\lambda_1 = \lambda_2$ . Inserting Eq. (2) into the time-dependent Schrödinger equation, and using the Hamiltonian in Eq. (1) leads to a system of coupled differential equations for the expansion coefficients:

$$\partial_t C_\lambda^e(t) = -i\Delta\omega_\lambda C_\lambda^e(t) - i\sqrt{2} \sum_{\lambda'} g_{\lambda'} C_{\lambda\lambda'}^g(t), \quad (3a)$$

$$\partial_t C_{\lambda_1\lambda_2}^g(t) = -i(\Delta\omega_{\lambda_1} + \Delta\omega_{\lambda_2}) C_{\lambda_1\lambda_2}^g(t) - \frac{i}{\sqrt{2}} \left( g_{\lambda_1}^* C_{\lambda_2}^e(t) + g_{\lambda_2}^* C_{\lambda_1}^e(t) \right). \quad (3b)$$

For a one-dimensional waveguide, such as the photonic crystal line defect in Fig. 1, it is reasonable to choose a frequency span where the emitter couples to only two waveguide modes propagating in opposite directions. In this case, the mode index  $\lambda$  labels modes described by a wavenumber  $k$ , having only a single polarisation, and where a positive or negative value of  $k$  implies a waveguide mode propagating to the right or left, respectively. With these assumptions, the sum over all modes in the waveguide reduces to  $\sum_\lambda = \lim_{L \rightarrow \infty} (L/2\pi) \int_{-\infty}^{\infty} dk$ , with  $L$  being the length of the 1D waveguide, and  $2\pi/L$  the spacing between the modes in reciprocal space. By defining continuous mode versions of the discrete functions and variables in Eqs. (3b),  $C^g(k, k', t) = \lim_{L \rightarrow \infty} (L/2\pi) C_{\lambda\lambda'}^g(t)$ ,  $C^e(k, t) = \lim_{L \rightarrow \infty} \sqrt{(L/2\pi)} C_\lambda^e(t)$ ,  $g(k) = \lim_{L \rightarrow \infty} \sqrt{(L/2\pi)} g_\lambda$ ,  $\Delta\omega(k) = \Delta\omega_\lambda$ , we have

$$\partial_t C^e(k, t) = -i\Delta\omega(k) C^e(k, t) - i\sqrt{2} \int_{-\infty}^{\infty} dk' g(k') C^g(k, k', t), \quad (4a)$$

$$\begin{aligned} \partial_t C^g(k_1, k_2, t) = & -i[\Delta\omega(k_1) + \Delta\omega(k_2)] C^g(k_1, k_2, t) \\ & - \frac{i}{\sqrt{2}} [g^*(k_1) C^e(k_2, t) + g^*(k_2) C^e(k_1, t)]. \end{aligned} \quad (4b)$$

By discretizing the  $k$ -continuum of modes, Eqs. (4a) and (4b) constitute a system of coupled linear differential equations; for certain input pulse shapes they can be solved analytically [27], but in general we solve them numerically. We note that in contrast to the linear nature of Eqs. (4a) and (4b), the Heisenberg equations of motion for the system operators used in the scattering matrix approach result in a set of coupled nonlinear differential equations, whose solution must instead be obtained using, e.g. the input–output formalism [22].

Within the Wigner-Weisskopf theory, the spontaneous emission rate of the emitter is given by  $\Gamma = \sum_\lambda 2\pi |g_\lambda|^2 \delta(\omega_\lambda - \omega_0)$ , and is typically of the order  $\sim 10^9 - 10^{10} \text{ s}^{-1}$  for quantum dots [31]; this is much less than the optical carrier frequencies of the pulses, which are typically of the order  $\omega_0 \sim 10^{15} \text{ s}^{-1}$ . Furthermore, by assuming a smooth dispersion curve for the waveguide modes, e.g. as shown in Fig. 1, the waveguide dispersion may be linearized around  $\omega_0$ , giving  $\Delta\omega(k) \approx v_g(|k| - k_0)$  with the group velocity  $v_g = (\partial\omega/\partial k)|_{k=k_0}$ .

## 2.2. Two-photon input state

Eqs. (4a) and (4b) can in principle be solved for any initial state of the total system containing two excitations. The case of a single exponentially shaped pulse scattering on an already excited TLE has been considered using a similar approach in Refs. [27, 32]. We build on these results by considering two optical pulses in the initial state, and investigate their scattering on the TLE

for various pulse widths and separations. The two-photon input states can be experimentally produced using, for example, parametric down-conversion, as has been demonstrated [34, 35, 36]. In general, such a process creates two correlated photons, but the properties of the down-conversion crystal can be modified in such a way that uncorrelated photons are produced [37].

We write the general form of a two-photon state as

$$|\beta\rangle = \frac{1}{\sqrt{2}} \int_{-\infty}^{\infty} dk \int_{-\infty}^{\infty} dk' \beta(k, k') a^\dagger(k) a^\dagger(k') |0\rangle, \quad (5)$$

with  $\beta(k, k')$  the two-photon wavepacket given in two-dimensional  $k$ -space. The bosonic nature of the photons implies symmetry of the two-photon wavepacket,  $\beta(k, k') = \beta(k', k)$ , and the normalisation condition is then  $\langle\beta|\beta\rangle = \int_{-\infty}^{\infty} dk \int_{-\infty}^{\infty} dk' |\beta(k, k')|^2 = 1$ . If we assume an initial condition corresponding to two photons described by Eq. (5), by comparison with Eq. (2) we find the corresponding initial conditions for the wavefunction coefficients  $C^e(k, 0) = 0$  and  $C^g(k, k', 0) = \beta(k, k')$ .

We write a general symmetric two-photon Gaussian state as  $\beta(k, k') = K [\beta_0(k, k') + \beta_0(k', k)]$  with

$$\beta_0(k, k') = f(k - k_{p,1} + k' - k_{p,2}) \xi_1(k) \xi_2(k'), \quad (6)$$

where  $\xi_i(k) = \sigma_i^{-1/2} \pi^{-1/4} \exp[-iz_{0,i}(k - k_{p,i}) - (k - k_{p,i})^2/(2\sigma_i^2)]$  is a Gaussian single-photon wavepacket with  $\sigma_i$  describing the spectral width,  $z_{0,i}$  the initial position of the pulse center, and where positive and negative  $k_{p,1}$  or  $k_{p,2}$  correspond to wavepackets propagating to the right and left respectively.  $K$  is a normalization parameter, and  $f(k, k')$  is a function describing phase matching, which for simplicity may be assumed to be a Gaussian,  $f(k) = \exp[-k^2/2\sigma_p^2]$  [38]. The correlation between the two photons is described by the parameter  $\sigma_p$ , which for parametric down-converted photons corresponds to the bandwidth of the pump laser [38]. The correlation parameter  $\sigma_p$  is inversely proportional to the correlation length between the photons, and thus  $\sigma_p \rightarrow \infty$  corresponds to fully uncorrelated photons, and in such a case  $\beta_0(k, k')$  factorizes into two single-photon wavepackets. We also define the real-space representation of the two-photon wavepacket by the Fourier transform

$$\beta(z, z') = \frac{1}{2\pi} \int_{-\infty}^{\infty} dk \int_{-\infty}^{\infty} dk' \beta(k, k') e^{ikz + ik'z'}. \quad (7)$$

In addition to the two-photon wavepacket, described by the functions  $\beta(k, k')$  and  $\beta(z, z')$ , it is also useful to define the expectation value of the photon density at a time  $t$  and position  $z$  as  $N(z, t) = \langle\psi(t)|a^\dagger(z)a(z)|\psi(t)\rangle$ , where  $a(z) = (2\pi)^{-1/2} \int dk a(k) e^{ikz}$  annihilates a photon at position  $z$ . This function has units of  $m^{-1}$ , and describes the distribution of energy in the waveguide. In terms of the wavefunction coefficients its explicit form is given by

$$N(z, t) = 2 \int_{-\infty}^{\infty} dk \left| \frac{1}{\sqrt{2\pi}} \int_{-\infty}^{\infty} dk' C^g(k, k', t) e^{ik'z} \right|^2 + \left| \frac{1}{\sqrt{2\pi}} \int_{-\infty}^{\infty} dk C^e(k, t) e^{ikz} \right|^2, \quad (8)$$

and since a lossless system is assumed, the number of excitations is conserved and we find  $\int_{-\infty}^{\infty} dz N(z, t) = 2$  at all times.

To gain some intuition as to how these three descriptions of the two-photon state appear, we first consider three different input states in the waveguide containing no TLE (such that wavepackets propagate along the waveguide but no other dynamics are present). The three rows in Fig. 2 correspond to the absolute value of the initial real-space photon wavepacket  $|\beta(z, z')|$ , the initial  $k$ -space wavepacket  $|\beta(k, k')|$ , and the photon density as a function of time  $N(z, t)$ , for

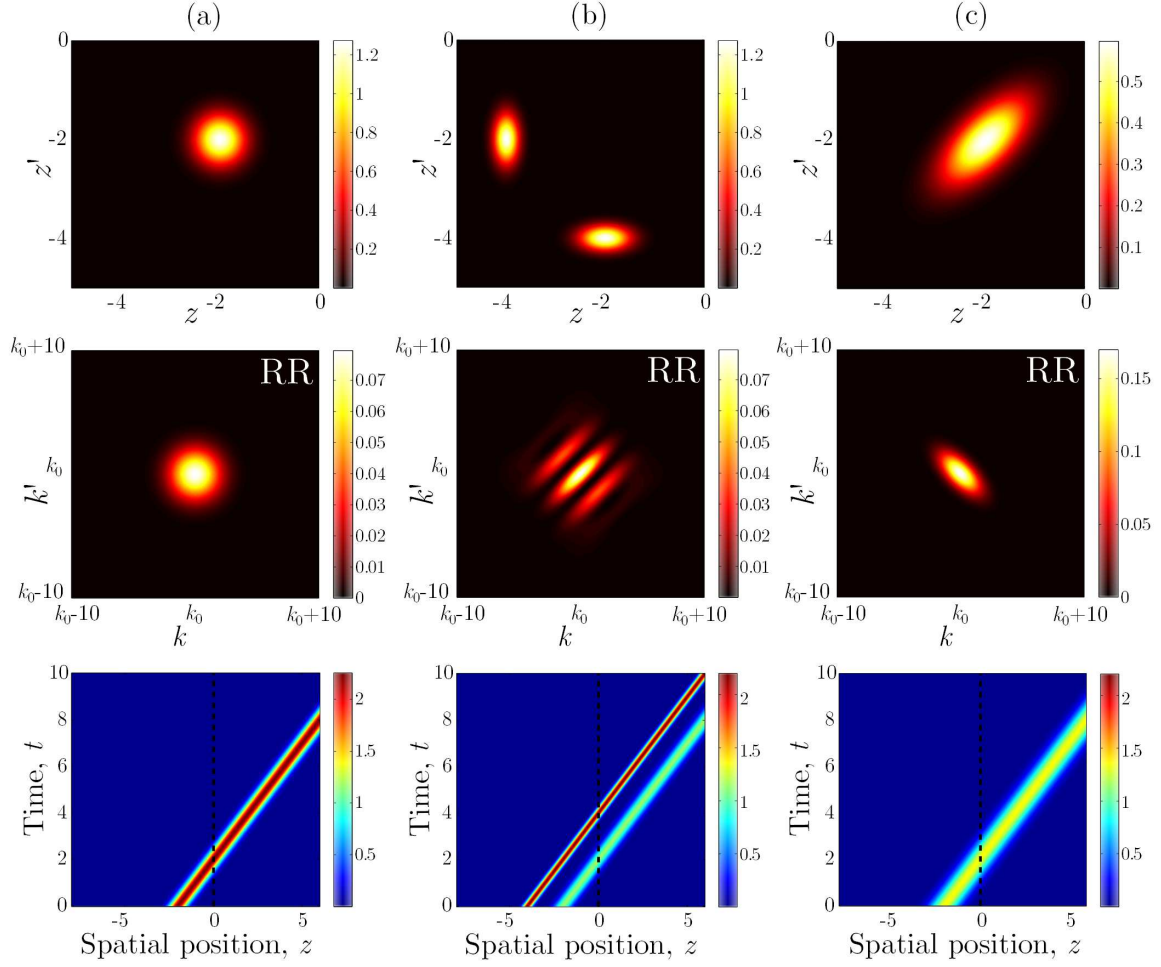


**Figure 2.** Absolute value of the two-photon wavepacket in real space,  $|\beta(z, z')|$  (upper row), in reciprocal space,  $|\beta(k, k')|$  (middle row), and the photon density  $N(z, t)$  (lower row) for three different two-photon states, and with no emitter positioned in the waveguide. The three columns correspond to initial photonic states which are co-propagating coincident uncorrelated pulses of equal width ( $\sigma_1 = \sigma_2 = 2$ ,  $z_{0,1} = z'_{0,2} = -2$ , and  $\sigma_p \rightarrow \infty$ , column (a)), uncorrelated spatially separated pulses of unequal widths ( $\sigma_1 = 2$ ,  $\sigma_2 = 4$ ,  $z_{0,1} = -2$ ,  $z'_{0,2} = -4$ , and  $\sigma_p \rightarrow \infty$ , column (b)), and coincident highly correlated pulses of equal width ( $\sigma_1 = \sigma_2 = 2$ ,  $z_{0,1} = z'_{0,1} = -2$ , and  $\sigma_p = (3/4)\sigma_1$ , column (c)).

input states which correspond to two coincident uncorrelated photons of equal width (column a), two spatially separated uncorrelated photons of different width (column b), and two coincident highly-correlated photons (column c). We note that in comparing columns (a) and (b), the separated nature of the two pulses in (b) is clearly visible, as too is the inequality of the two pulse widths, as is evident from the elliptical shape of the wavepacket amplitudes in the top row. We also see oscillations appearing the  $k$ -space representation for the spatially separated pulses in column (b). These oscillations have a period  $|z_{0,1} - z_{0,2}|^{-1}$  and are a signature of interference between the two separated pulses. For the correlated pulses in column (c) we see that the wavepacket is elongated along the diagonal line  $z = z'$  in real-space, and along the  $k = -k'$

direction in frequency space. This means that position measurements of the two photons will share positive correlations, whereas frequency measurements will be anti-correlated. Finally, we note that the photon density plots in the lower row provide us with an overall picture of the dynamics for all times, but do not capture all the features present in the photon wavepackets.

### 3. Co-propagating pulses

We now turn to the main focus of this work, and consider the evolution of the two photon state as it scatters on a TLE placed inside the waveguide. In order to solve Eqs. (4a) and (4b), we discretize the continuum of waveguide modes and numerically solve the resulting finite set of differential equations. In the following calculations we assume frequency-independent coupling constants,  $g(k) = g$ , which is well justified owing to the assumption that the TLE linewidth is narrow compared to the carrier frequency of the wavepackets; in general, the approach we use allows for frequency dependent coupling constants, which could be relevant, for example, when considering coupling to optical cavities [39]. Convergence tests were performed by comparison with the well-known scattering properties of a single photon [20], and to analytical expressions for the induced TLE excitation probability obtained by solving Eqs. (4a) and (4b) for a two-photon Gaussian input pulse (using the method of Refs. [26, 27]). Our results in the long-time limit agree with the scattering matrix approach of Refs. [22, 25]. In all plots, parameters with units of time or length are normalized to  $\Gamma^{-1}$  and  $v_g/\Gamma$  respectively. A pulse with a spectral width of  $\sigma = 1$  thus corresponds to a spatial width of  $v_g/\Gamma$  and a temporal width of  $\Gamma^{-1}$ . Finally, for plotting in  $z$ -space, we used a frequency of  $\omega_0 = 10^{15} \text{ s}^{-1}$ .

#### 3.1. Scattering dynamics

As an illustrative example of two-photon scattering, we first consider the scattering of two identical, coincident and uncorrelated single-photon pulses with carrier frequencies resonant with the TLE. Except for the inclusion of a TLE here, the input is identical to that of column (a) in Fig. 2; both photons are initially located left of the TLE,  $z_{0,1} = z_{0,2} < 0$ , and propagate to the right,  $k_{p,1} = k_{p,2} > 0$ . On the left of Fig. 3 we show the photon density  $N(z, t)$ , which represents the expectation value of position measurements of the two photons over many scattering events. We see that part of the energy is transmitted, and part is reflected. On the incoming side of the emitter ( $z < 0$ ), a standing wave pattern is clearly visible, which is a result of interference between the incoming and reflected part of the pulse.

The upper row on the right shows the evolution of the spatial wavepacket at three representative times, corresponding to the onset of the scattering  $t = 3.0$ , during the scattering  $t = 4.7$ , and in the post-scattering long-time limit  $t = 10.0$ . We notice that after the scattering event, both photons clearly propagate away from the TLE as expected. Additionally, the scattered state contains all possible spatial configurations of the photons: both being in the region right of the TLE, “ $RR$ ”, one on each side, “ $LR$ ”, and both photons to the left of the TLE, “ $LL$ ”. An equivalent conclusion may also be drawn from the wavepacket in  $k$ -space as shown in the lower row of Fig. 3, where the scattered field has components propagating in the “ $RR$ ”, “ $LR$ ”, or “ $LL$ ” directions. Due to the bosonic nature of the photons, the configurations “ $LR$ ” and “ $RL$ ” cannot be distinguished. At early times, e.g. at  $t = 3.0$  in Fig. 3, the scattering is dominated by single photon processes, which can be seen by the fact that the two-photon wavepacket is elongated along the  $k$  and  $k'$  axes. This means that only a single photon has been broadened by its interaction with the TLE emitter, whilst the other remains unchanged. At larger times, features of two-photon scattering processes appear, which can be seen by the more complex shapes of the two-photon wavepackets. We discuss these features in more detail below.

It is interesting to compare the scattering dynamics in Fig. 3 with the case of two pulses which are sufficiently separated in space such that the TLE excitation induced by the first pulse has essentially decayed before the arrival of the second pulse. This is shown in Fig. 4, and in this

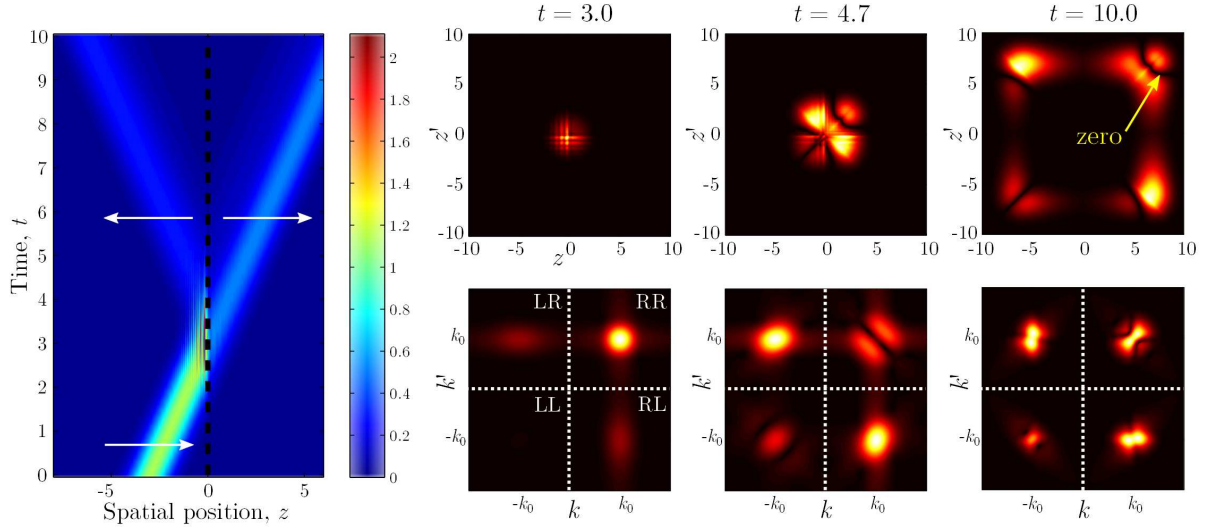


**Figure 3.** Left: Photon density,  $N(z, t)$  for an initially uncorrelated ( $\sigma_p \rightarrow \infty$ ) coincident two-photon state scattering on an emitter placed at  $z = 0$ , using widths  $\sigma_1 = \sigma_2 = 1$  and initial centre positions  $z_{0,1} = z_{0,2} = -3$ . The position of the emitter at  $z = 0$  is indicated by the black dashed line. Right: Absolute value of the two-photon wavepacket shown at three representative times during the scattering event, both in  $z$ -space (upper row) and  $k$ -space (lower row). In the  $k$ -space plots, we show only the regions centred around  $k, k' = \pm k_0$ , which we label *LL* (origin  $(-k_0, -k_0)$ ), *RR* (origin  $(k_0, k_0)$ ), *LR* (origin  $(-k_0, k_0)$ ), and *RL* (origin  $(k_0, -k_0)$ ).

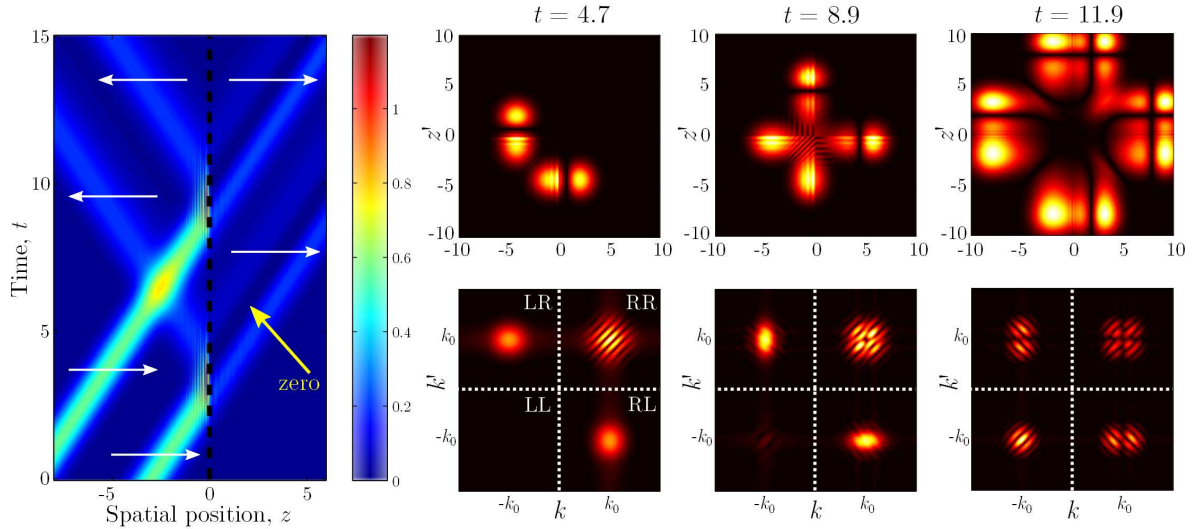


**Figure 4.** Left: Photon density,  $N(z, t)$  for an uncorrelated ( $\sigma_p \rightarrow \infty$ ) two-photon state scattering on the emitter placed at  $z = 0$ , using widths  $\sigma_1 = \sigma_2 = 1$  and initial centre positions  $z_{0,1} = -3$  and  $z_{0,2} = -9$ . The position of the emitter at  $z = 0$  is indicated by the black dashed line. Right: Absolute value of the two-photon wavefunction shown at three different times during the scattering event, both in  $z$ -space (upper row) and  $k$ -space (lower row). In the  $k$ -plots, only the regions centred around  $k, k' = \pm k_0$  are shown.



case the scattering behaviour resembles two ‘copies’ of the single-photon scattering case [20]. Even though the carrier frequency of the pulse is resonant with the TLE, a non-zero transmission is obtained in this single-photon scattering limit because of the finite temporal widths of the input pulses. These features are in contrast to the case in which a spectrally narrow continuous wave pulse is incident on the emitter, which gives zero transmission on resonance because of destructive interference between the scattered and input fields [17, 18]. In this single-photon scattering limit, the TLE fully reflects frequency components of the incoming pulse which are close to the TLE resonance, as no two-photon processes are apparent. Hence, the spectrum of the transmitted pulse does not contain components at these frequencies, see e.g. the spectrum in Fig. 4 at  $t = 11.9$ . This is in contrast to the coincident case in Fig. 3, where two-photon processes allow for transmission of pulse components close to the TLE resonance.

During the initial phase of the scattering, the  $k$ -space wavefunctions in both Fig. 3 and Fig. 4 broaden and demonstrate interaction with states which are detuned from the TLE by several TLE linewidths. This may be seen at times  $t = 3.0$  and  $t = 4.7$  in Fig. 3, but these frequencies do not appear in the final scattered state at  $t = 10.0$ . This phenomenon may be understood as arising from the energy-time uncertainty relation, as processes taking place at short times allow for larger uncertainties in energy. Lastly, for the case of spatially separated pulses in Fig. 4, a dip is present in the transmitted waveguide excitation. This feature is a consequence of destructive interference between the initial photon wavepacket and the emitted photon, and manifests in the form of a dip in the spectrum of the transmitted pulse at the emitter transition frequency [20]. This dip is not apparent in the plot of  $N(z, t)$  for the case of two initially coincident pulses in Fig. 3, but is present in the two-photon wavepacket in  $z$ -space as indicated for  $t = 10.0$ . Physically, it means that a photon may be detected at a position corresponding to the dip, but *if* the first photon is detected there, the probability of detecting the second photon at that position is zero, exemplifying that the single-photon scattering features manifest themselves in two-photon scattering, although they may not be apparent from the photon density  $N(z, t)$ .

To summarise, we have illustrated the full scattering dynamics of two photons on a TLE by calculating the total system state at all times. For well-separated uncorrelated single-photon pulses, the dynamics may be well approximated by the single-photon results [20]. As the displacement between the pulses becomes smaller, non-trivial dynamics can be induced due to the saturation of the TLE. The approach we use here naturally accommodates this regime of two photon scattering.

### 3.2. Transmission and reflection properties

In order to investigate the transmission properties of the TLE, we consider the relative number of photons propagating to the left and right during the scattering process. We can calculate the total number of photons propagating to the right as

$$N_{\text{R}}(t) = \int_0^{\infty} dk \langle \psi(t) | a^\dagger(k) a(k) | \psi(t) \rangle \quad (9)$$

$$= 2 \int_0^{\infty} dk \int_{-\infty}^{\infty} dk' |C^{\text{g}}(k, k', t)|^2 + \int_0^{\infty} dk |C^{\text{e}}(k, t)|^2, \quad (10)$$

while the total number propagating to the left,  $N_{\text{L}}(t) = \int_{-\infty}^0 dk \langle \psi(t) | a^\dagger(k) a(k) | \psi(t) \rangle$ , is given by a similar expression with the integration range over  $k$  changed to  $[-\infty, 0]$ . The excitation probability of the TLE is given by

$$P_{\text{e}}(t) = \langle \psi(t) | c^\dagger c | \psi(t) \rangle = \int_{-\infty}^{\infty} dk |C^{\text{e}}(k, t)|^2, \quad (11)$$

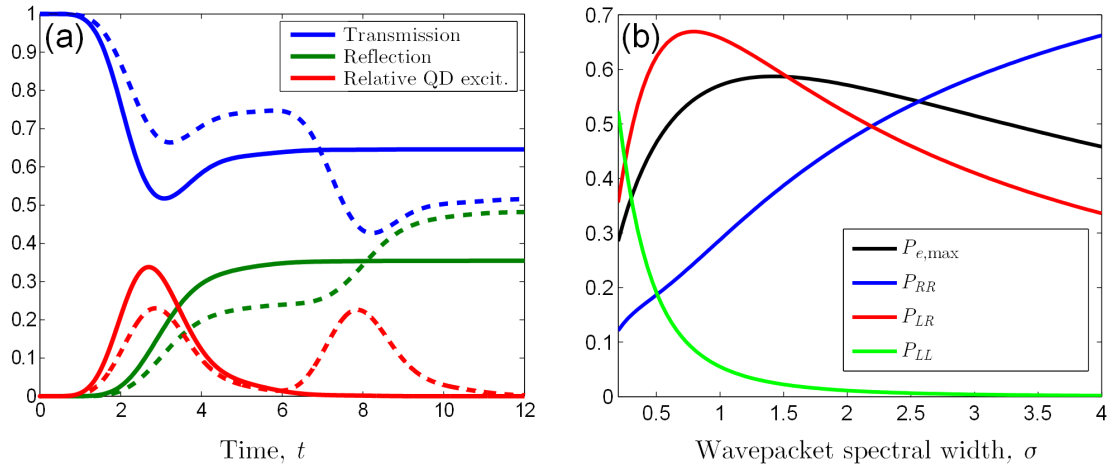


**Figure 5.** (a) Transmission  $T_R(t)$  (blue) and reflection  $T_L(t)$  (green), together with relative TLE excitation,  $P_e(t)/2$  (red), for parameters corresponding to the two cases of perfectly overlapping (solid) and non-overlapping (dashed) pulses shown in Figs. 3 and 4 respectively. (b) Maximum TLE excitation and the directional scattering probabilities as a function of the wavepacket  $k$ -space width,  $\sigma$ , for two coincident but uncorrelated, single-photon pulses with the same width and carrier frequency, resonant with the TLE transition.

and normalization of the total state ensures  $N_R(t) + N_L(t) + P_e(t) = 2$ ; there is a total of two excitations in the system at all times. We therefore define the *relative* transmission to the right and left as  $T_R(t) = N_R(t)/2$  and  $T_L(t) = N_L(t)/2$ .

In Fig. 5(a) we show the left and right transmission coefficients, together with the TLE excitation as a function of time, for the two cases of perfectly overlapping (solid) and non-overlapping pulses (dashed) introduced in Figs. 3 and 4 respectively. From these plots a clear reduction in the reflective nature of the TLE when the two pulses are coincident is evident, clearly illustrating that the first photon induces partial transparency in the TLE, minimising the interaction between the TLE and the second photon.<sup>1</sup> Also evident is a temporal delay between excitation of the TLE and the accumulation of the reflected field, demonstrating non-instant scattering due to the finite decay rate of the TLE.

The transmission and reflection coefficients do not contain information regarding scattering-induced correlations between the photons, and to that end we define scattering probabilities for the three possible directional outcomes of the scattering process. In the long-time limit, the probability that both photons propagate to the right is given by

$$P_{RR} = \frac{1}{2} \lim_{t \rightarrow \infty} \int_0^\infty dk \int_0^\infty dk' \langle \psi(t) | a^\dagger(k) a^\dagger(k') a(k') a(k) | \psi(t) \rangle \quad (12)$$

$$= \lim_{t \rightarrow \infty} \int_0^\infty dk \int_0^\infty dk' |C^g(k, k', t)|^2, \quad (13)$$

while  $P_{LL}$  is given by a similar expression with the integration ranges changed to  $[-\infty, 0]$ . The

<sup>1</sup> Due to the symmetry, the maximum achievable TLE excitation for a single-pulse excitation from a single side is  $1/2$ , which is obtained for a pulse with a temporal shape which is exactly the inverse of a pulse emitted by the TLE [40]. Such a pulse would render the TLE completely transparent.

probability of having one photon travelling in each of the two directions is

$$P_{LR}(t) = 2 \lim_{t \rightarrow \infty} \int_{-\infty}^0 dk \int_0^{\infty} dk' |C^g(k, k', t)|^2. \quad (14)$$

The scattering probabilities  $P_{RR}$ ,  $P_{LR}$ , and  $P_{LL}$  are thus obtained by integrating the two-photon wavepacket over the corresponding quadrant(s) in Fig. 3 or Fig. 4 in either  $z$ - or  $k$ -space.

At long times well past the scattering event, when the TLE has fully decayed to its ground state, the probabilities we have defined satisfy  $P_{RR} + P_{LL} + P_{LR} = 1$ . In contrast to the quantities  $T_R$  and  $T_L$ , the probabilities  $P_{RR}$ ,  $P_{LL}$ , and  $P_{LR}$  contain information regarding the directional correlation between the individual photons. The correlations depend crucially on the width of the photon wavepacket, as well as the initial emitter excitation. To investigate this, Fig. 5(b) shows the directional scattering probabilities as a function of the width of two equal coincident input pulses, together with the maximal emitter excitation,  $P_{e,\max}$ . The scattering of monochromatic pulses (infinitely small  $\sigma$ ) is well-known [17, 18]; all of the pulse is reflected when the carrier frequency is resonant with the emitter transition, agreeing with our results here in the limit of a small  $\sigma$ . Here the TLE excitation remains low due to the low optical power in the pulse. Spectrally broad pulses have a small overlap with the TLE in  $k$ -space, resulting in a small degree of interaction and thus also a low value of  $P_{e,\max}$  and a high value of  $P_{RR}$ . The largest  $P_{e,\max}$  is obtained for  $\sigma \sim \Gamma/v_g$  which is also the parameter regime where  $P_{LR}$  dominates. This occurs when the spectral overlap between the wavepacket of the input state and the TLE emission spectrum is large.

#### 4. Counter-propagating pulses

We now turn to the case where the TLE is illuminated by two counter-propagating single-photon pulses, one photon from each side of the TLE. The corresponding waveguide excitation dynamics is shown in Fig. 6, for excitation pulses with a carrier frequency resonant with the TLE transition energy. Due to the symmetry of the scattering problem around  $z = 0$ , the expectation value of the photon density is the same for the left and right propagating components of the pulse.

Closer inspection of the two-photon wavepacket on the right of Fig. 6 reveals interesting features regarding the induced correlations. We see that  $P_{LR}$  is much smaller than  $P_{RR}$  and  $P_{LL}$ . This indicates a strong directional correlation between the two scattered photons as the final state suggests both photons will be measured propagating in the same direction with high probability. We note that this property cannot be inferred from the photon density plot. This phenomenon is analogous to the well-known two-photon interference which gives rise to the Hong-Ou-Mandel dip, wherein two identical photons impinging from opposite sides of an optical beam-splitter coalesce and are measured in the same output arm [41]. In the present case, however, the effect is only partial due to the non-zero spectral width of the input pulses and the TLE saturation, and as a consequence  $P_{LR}$  is not zero. This beam splitter-like effect has been observed in Ref. [42] for coupled optical waveguides described by a tight-binding model between the individual sites.

##### 4.1. Induced Correlations

We now turn our attention to the correlations induced in the two-photon-state as a result of the scattering process. First, it is important to establish in which degrees of freedom the photons can be correlated. We distinguish between two correlation types, which we refer to as ‘directional’ and ‘modal’. Directional correlations are those present in measurement statistics acquired from detecting the *direction of propagation* of each of the two photons, and are captured by the quantities  $P_{ij}$  for  $\{i, j\} \in \{R, L\}$ . If the propagation direction of one photon depends on the measured propagation direction of the other, the two are said to have directional correlations.

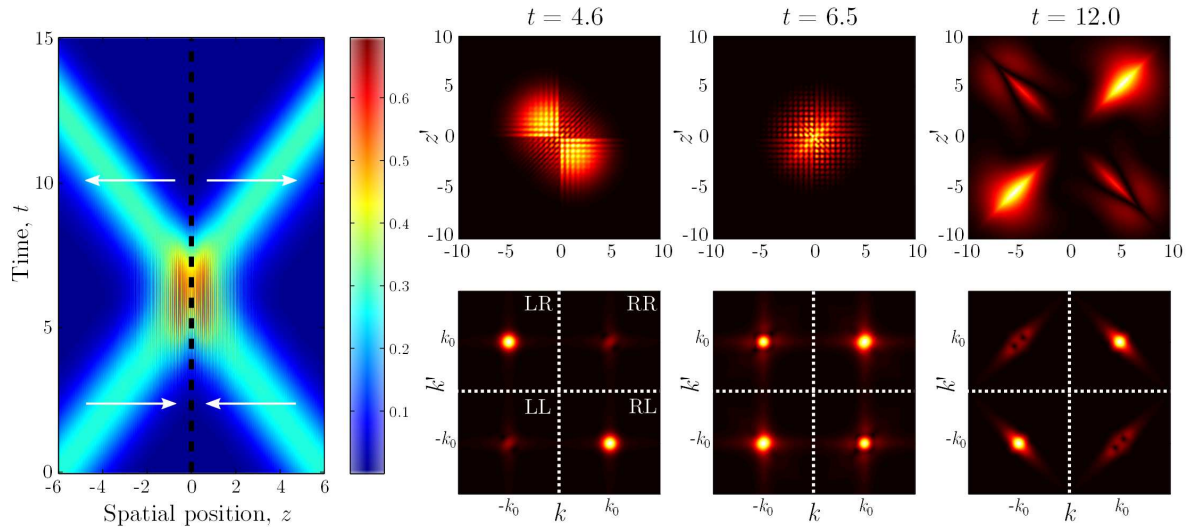


**Figure 6.** Left: Photon density,  $N(z, t)$  for an initially uncorrelated ( $\sigma_p \rightarrow \infty$ ) two-photon state scattering on the emitter placed at  $z = 0$ , using pulse widths  $\sigma_1 = \sigma_2 = 0.5$  and initial centre positions  $z_{0,1} = z_{0,2} = -6$ . The position of the emitter at  $z = 0$  is indicated by the dashed black line. Absolute value of the two-photon wavefunction shown at three different times during the scattering event, both in  $z$ -space (upper row) and  $k$ -space (lower row). In the  $k$ -space plots, only the intervals centred at  $k, k' = \pm k_0$  are shown.

Modal correlations, on the other hand, are concerned with measurement statistics obtained when detecting the *position* of each photon, assuming a given configuration of propagation directions. These modal correlations are contained in the correlation parameter  $\sigma_p$ , defined for the input state in Eq. (6). Modal correlations are more traditionally described in terms of the well-known second order  $g^{(2)}$  correlation function [43], which is typically employed when describing intensity correlations. A generic two-photon state may be correlated according to one of these measures, but fully uncorrelated in the other. Fig. 2(c) shows an example of such a state. The elliptical shape of the wavepacket in real-space is a signature of modal correlations, but the state can have no directional correlations, since both photons are propagating to the right.

The scattering of co-propagating photons shown in Fig. 6 induces strong directional correlations. Modal correlations are also induced, as can be seen from the elliptical shape of the wavefunction in  $z$ -space and  $k$ -space, meaning that the emitted photons are anti-correlated in  $k$ -space and correlated in  $z$ -space. This can be further appreciated by comparison with the state shown in Fig. 2(c), which was defined to have modal correlations. The induced anti-correlation in  $k$ -space can be understood as a four-wave mixing process, where elastic scattering of two photons of almost identical energy results in one photon with higher energy and one with lower energy. This gives rise to the elliptical shape of the wavefunction in  $k$ -space, cf. the spectrum in Fig. 6 at  $t = 12.0$ . The correlation in  $z$ -space implies a larger probability of detecting the second photon spatially close to the first, i.e. photon bunching. Modal correlations such as these are not present in the scattered state from a conventional linear optical beam splitter; the modal entanglement observed here is caused by a non-linear scattering process between the incoming and emitted photons, which is mediated by the excitation of the TLE.

#### 4.2. Induced entanglement

In order to relate the induced quantum correlations in the photonic state to the TLE excitation dynamics, we require a measure of the induced correlations, which can be facilitated by entanglement theory. There are several proposals in the literature of how to quantify the degree of entanglement (quantum correlations) between individual subsystems [44, 45, 46], particularly for distinguishable systems each of which may be in one of only two states, e.g. two spatially separated spin-half particles. These measures include the fidelity, the concurrence, the negativity, and the entropy of entanglement [7], each of which has a different operational meaning, and may be more or less appropriate given the problem at hand. For two indistinguishable particles e.g. two bosons in the same two-photon Hilbert space, extensions to the distinguishable case have to be made [47, 48, 49]. If the indistinguishable bosons can each occupy more than two states, as is the case for the state expressed by Eq. (2) (where the number of states is equal to the dimension of each particle sub-Hilbert space), there are fewer ways to quantify the entanglement. Among these is the von Neumann entropy of the reduced single-particle density matrix [48, 50], which quantifies the modal entanglement by the degree to which the state of the second photon is affected by a  $k$ -space measurement on the first.

In order to explore the extent to which our system behaves as a beam-splitter, we quantify the amount of directional entanglement present in the scattered state. To do this, the two-photon state may be projected onto a two-dimensional Hilbert space with each photon being in either a left or a right propagating state, giving three basis states,  $|LL\rangle$ ,  $|LR\rangle$ , and  $|RR\rangle$ . This projected system is identical to the case of two indistinguishable two-state particles discussed above, for which the entanglement may be quantified by the fidelity, i.e. by comparison to a maximally entangled state. We focus here only on entangled states with a different number of particles in each direction and thus compare to two of the four Bell-states only,

$$|\Phi^\pm\rangle = \frac{1}{\sqrt{2}} [ |LL\rangle \pm |RR\rangle ]. \quad (15)$$

For pure states as in Eq. (2), the fidelities with respect to the maximally entangled states are defined as the overlap between the scattered state and the maximally entangled state,  $F^\pm = |\langle \Phi^\pm | \psi \rangle|^2$  [7]. The fidelities exceed 1/2 only if  $|\psi\rangle$  is a non-classical state, and can therefore be interpreted as a measure of the directional entanglement.

For two identical photons scattering on the TLE from each side, as in Fig. 6, the input state has  $F^\pm = 0$ , as the overlap with the initial state  $|LR\rangle$  is zero. The fidelity for the scattered state is shown in Fig. 7 for varying widths of the input pulses. The correlated input state, where both photons have a larger probability of scattering on the TLE at the same time, leads to a smaller fidelity at the output than for two uncorrelated photons at the input. For the initially correlated states, such as that shown in in Fig. 2(c), the spectrum of the photons is tighter than the uncorrelated case in Fig. 2(a), but the spatial distribution is broadened, resulting in a lower probability of having both of the photons at the TLE at the same time; this decreases the induced correlations and correspondingly leads to a smaller fidelity..

In the limit of large  $\sigma$ , only a small fraction of the pulse interacts with the TLE, giving a fidelity which approaches zero. In the small  $\sigma$  limit, the incoming pulse is temporally broad, resulting in a low light intensity at the TLE position at all times, and hence, to a good approximation, the TLE remains in its ground state. As the TLE only induces non-linearities when it is excited, a two-photon packet with small  $\sigma$  scatters as if the two photons were scattering individually on the TLE, giving the scattered state  $|LR\rangle$ . We note that the maximum fidelity is obtained when the linewidth of the Gaussian input pulses is comparable with the decay rate of the TLE. In this case excitation of the TLE is high, and a highly directionally entangled state is produced.

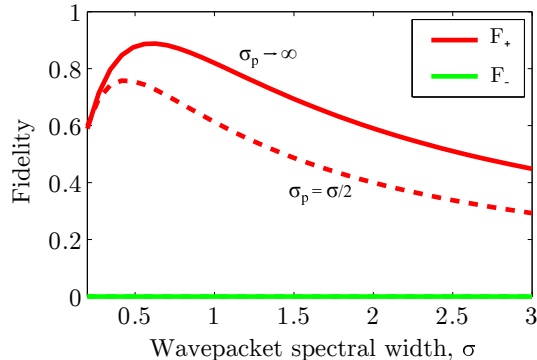


**Figure 7.** Directional entanglement, quantified by the fidelity, plotted versus the spectral width of the photon wavepacket. Here we consider two identical, single-photon wavepackets impinging on the TLE from each side, initially equidistant from the TLE, and both being resonant with the TLE transition (i.e. the conditions are the same as those of Fig. 6 for which  $\sigma_1 = \sigma_2 = 0.5$  and  $\sigma_p \rightarrow \infty$ ). Cases of initially uncorrelated states,  $\sigma_p \rightarrow \infty$ , and spatially correlated states,  $\sigma_p = \sigma_1/2$  are shown, and the wavepacket widths are always equal  $\sigma_1 = \sigma_2 = \sigma$ .

## 5. Conclusion

In conclusion, we have developed a wavefunction approach to study the scattering of two photons on a two-level emitter in a one-dimensional waveguide. Our method benefits from the simple mathematical form, and provides the full temporal dynamics of the scattering event, as well as a detailed description of the scattering-induced correlations. For co-propagating pulses, we saw that the excitation of the emitter strongly influences its transparency. This results in transmission and reflection coefficients which depend sensitively on the separation between the two input pulses. For counter-propagating pulses, the emitter–waveguide system shows beam-splitter like features, generating directional correlations and entanglement in the scattered two-photon state, occurring most strongly when the emitter excitation is largest. Unlike a conventional linear optical beam-splitter, however, the finite decay rate of the emitter introduces non-linearities which manifest as additional bunching effects. Finally, we note that our model could be extended to more complicated scattering scenarios, such as several quantum dots with possibly additional levels [51, 52]. The numerical approach we use also allows for the investigation of the role of waveguide dispersion, as well as non-Markovian coupling to the scattering object by including frequency-dependent coupling coefficients in the system, which we plan to investigate in future work.

## 6. Acknowledgments

This work was supported by Villum Fonden via the Centre of Excellence NATEC, the Danish Council for Independent Research (FTP 10-093651) and by the European Metrology Research Programme (EMRP) via the project SIQUTE (Contract No. EXL02). The EMRP is jointly funded by the EMRP participating countries within EURAMET and the European Union.

## References

- [1] O’Brien J L, Furusawa A, and Vučković J 2009 *Nature Photonics* **3** 687-695
- [2] Claudon J, Bleuse J, Malikdynamik N S, Bazin M, Jaffrennou P, Gregersen N, Sauvan C, Lalanne P, and Gérard J-M 2010 *Nature Photonics* **4** 174-177
- [3] Gisin N and Thew R 2007 *Nature Photonics* **1** 165-171
- [4] Giovannetti V, Lloyd S, and Maccone L 2004 *Science* **306** 1330-1336

- [5] Knill E, Laflamme R, and Milburn G J 2001 *Nature* **409** 46-52
- [6] Kok P, Munro W J, Ralph T C, Dowling J P, and Milburn G J 2007 *Reviews of Modern Physics* **79** 135-174
- [7] Kok P and Lovett B W 2010 *Introduction to Optical Quantum Information Processing* (Cambridge: Cambridge University Press)
- [8] Banin U, Cao Y W, Katz D, Millo O 1999 *Nature* **400** 542-544
- [9] Bayer M, Stern O, Hawrylak P, Fafard S, and Forchel A 2000 *Nature* **405** 923-926
- [10] Santori C, Fattal D, Vučković J, Solomon G S, and Yamamoto Y, 2002 *Nature* **419** 594-597
- [11] Chang D E, Sørensen A S, Demler E A, and Lukin M D 2007 *Nature Physics* **3** 807
- [12] Chen Y, Nielsen T R, Gregersen N, Lodahl P, and Mørk J 2010 *Phys. Rev. B* **81** 125431
- [13] Lund-Hansen T, Stobbe S, Julsgaard B, Thyrrestrup H, Sunner T, Kamp M, Forchel A, and Lodahl P 2008 *Phys. Rev. Lett.* **101** 113903
- [14] Yao P, Rao M, and Hughes S 2009 *Laser Photonics Rev.* **4** 499-516
- [15] Arcari M, Söllner I, Javadi A, Hansen S L, Mahmoodian S, Liu J, Thyrrestrup H, Lee E H, Song J D, Stobbe S, and Lodahl P 2014 *Phys. Rev. Lett.* **113** 093609
- [16] Surrente A, Gallo P, Felici M, Dwir B, Rudra A, and Kapon E 2009 *Nanotechnology* **20** 415205
- [17] Auffèves-Garnier A, Simon C, Gérard J-M, and Poizat J-P 2007 *Phys. Rev. A* **75** 053823
- [18] Shen J-T and Fan S 2009 *Phys. Rev. A* **79** 023837
- [19] Hughes S and Roy C 2012 *Phys. Rev. B* **85** 035315
- [20] Chen Y, Wubs M, Mørk J, and Koenderink A F 2011 *New Journal of Physics* **13** 103010
- [21] Shen J-T and Fan S 2007 *Phys. Rev. Lett.* **98** 153003
- [22] Fan S, Kocabas, S E, and Shen J-T 2010 *Phys. Rev. A* **82** 063821
- [23] Shen J-T and Fan S 2007 *Phys. Rev. A* **76** 062709
- [24] Shi T and Sun C P 2009 *Phys. Rev. B* **79** 205111
- [25] Zheng H, Gauthier D J, and Baranger H U 2010 *Phys. Rev. A* **82** 063816
- [26] Kojima K, Hofmann H F, Takeuchi S, and Sasaki K 2003 *Phys. Rev. A* **68** 013803
- [27] D. Valente and Y. Li and J. P. Poizat and J. M. Gérard and L. C. Kwek and M. F. Santos and A. Auffèves 2012 *New Journal of Physics* **14** 083029
- [28] Longo P, Schmitteckert P, and Busch K 2009 *Jour. of Optics A* **11** 114009
- [29] Moferdt M, Schmitteckert P, and Busch K 2013 *Optics Letters* **38** 3693-3695
- [30] Witthaut D, Lukin M D, and Sørensen A S 2012 *Europhysics Letters* **97** 50007
- [31] Stobbe S, Johansen J, Kristensen P T, Hvam J M, and Lodahl P 2009 *Phys. Rev. B* **80** 155307
- [32] Rephaeli E and Fan S 2012 *Phys. Rev. Lett.* **108** 143602
- [33] Hayat A, Ginzburg P, and Orenstein M 2008 *Nature Photonics* **2** 238-241
- [34] Cinelli C, Di Nepi G, De Martini F, Barbieri M, and Mataloni P 2004 *Phys. Rev. A* **70** 022321
- [35] Ostermeyer M, Korn D, Puhlmann D, Henkel C, and Eisert J 2009 *Journal of Modern Optics* **56** 1829-1837
- [36] Harder G, Ansari V, Brecht B, Dirmeier T, Marquardt C, and Silberhorn C 2013 *Optics Express* **21** 545-550
- [37] Grice W P, U'Ren A B, and Walmsley I A 2001 *Phys. Rev. A* **64** 063815
- [38] Wang K 2006 *J. Phys. B* **39** 293
- [39] Vahala K J 2003 *Nature* **424** 839-846
- [40] Rephaeli E, Shen J-T, and Fan S 2010 *Phys. Rev. A* **82** 033804
- [41] Hong C K, Ou Z Y, and Mandel L *Phys. Rev. Lett.* **59** 2044
- [42] Longo P, Cole J H, and Busch K 2012 *Optics Express* **20** 12326
- [43] Zheng H, Gauthier D J, and Baranger H U 2012 *Phys. Rev. A* **85** 043832
- [44] Vidal G and Werner R F 2002 *Phys. Rev. A* **65** 032314
- [45] Plenio M B and Virmani S 2007 *Quantum Information & Computation* **7** 1-51
- [46] Vedral V and Plenio M B 1998 *Phys. Rev. A* **57** 1619
- [47] Wiseman H M and Vaccaro J A 2003 *Phys. Rev. Lett.* **91** 097902
- [48] Ghirardi G and Marinatto L 2004 *Phys. Rev. A* **70** 012109
- [49] Eckert K, Schliemann J, Bruss D, Lewenstein M 2002 *Annals of Physics* **299** 88-127
- [50] Pakauskas R. and You L 2001 *Phys. Rev. A* **64** 042310
- [51] Witthaut D and Sørensen A S 2010 *New Journal of Physics* **12** 043052
- [52] Martens C, Longo P, and Busch K 2013 *New Journal of Physics* **15** 083019